

# Single mode fiber dislocation Mach-Zehnder interferometer cascaded with fiber Bragg grating for monitoring metal electrochemical corrosion\*

ZHANG Shuaibo, LIU Xiaoqi\*\*, WANG Zhi, and LIU Yange

Tianjin Key Laboratory of Micro-scale Optical Information Science and Technology, Institute of Modern Optics, Nankai University, Tianjin 300350, China

(Received 17 March 2023; Revised 30 March 2023)

©Tianjin University of Technology 2023

An optical fiber sensor composed of a dislocation Mach-Zehnder interferometer (MZI) cascaded with a fiber Bragg grating (FBG) is proposed, and it is used to monitor the electrochemical corrosion of metals in experiments. The dislocation interferometer is composed of two segments of single-mode fiber (SMF) and one segment of dislocation SMF. The contact surface is increased between the fiber and the environment, which helps to improve the interference sensitivity. The relationship between the dislocation amount and the refractive index sensitivity of the interferometer is discussed through simulation. In the experiment, the sensitivity of the interferometer reaches more than 10 000 nm/RIU, and the monitoring of metal electrochemical corrosion is also realized in 3.5% NaCl solution. The proposed measurement scheme has the advantages of small structure, low cost and high sensitivity. It has good prospects in chemical reaction monitoring.

**Document code:** A **Article ID:** 1673-1905(2023)11-0653-6

**DOI** <https://doi.org/10.1007/s11801-023-3048-3>

Metal corrosion happens around us all the time. Metal corrosion may damage the performance of metal instruments and cause harm to industrial production, so metal corrosion monitoring is very necessary<sup>[1-3]</sup>. In recent years, battery technology has been developed rapidly. The metal also acts as an electrode to cause electrochemical corrosion. It is very important to monitor electrode corrosion to evaluate battery characteristics<sup>[4,5]</sup>. In recent years, optical fiber sensor has attracted people's attention due to its small size, flexible shape, high sensitivity and anti-electromagnetic interference<sup>[6-9]</sup>. More optical fiber sensors can provide a good linear response to monitor the changes of the environment in real time, and have higher sensitivity, which makes them applicable to many aspects of life.

Metal corrosion monitoring is mainly divided into indirect measurement method and direct measurement method. The direct measurement method includes the quality method and the flatness measurement of the toilet surface. However, direct corrosion monitoring can't accurately characterize metal corrosion or be monitored in real time. Therefore, many indirect measurement methods have received more attention. In 2017, HU et al<sup>[2]</sup> proposed a fiber polarizer for sputtering Fe-C film on a single-mode fiber (SMF) polished on the side of the fiber. Monitoring of steel corrosion is realized by measuring

the change of extinction ratio of TE and TM modes. In the same year, CHEN et al<sup>[10]</sup> studied the corrosion process of metal Fe by plating Fe-C film on the surface of long-period fiber grating, in which the metal film is deposited on the fiber core. As the corrosion of the metal film occurs, the relationship between the grating resonance peak and the corrosion degree is compared to determine the corrosion process. In 2018, LAO et al<sup>[4]</sup> studied the corrosion monitoring of the metal plates during the charging and discharging process of the capacitor plates with the inclined Bragg grating on the metal surface. HOSHI et al<sup>[11]</sup> used non-contact wide frequency range electrochemical impedance measurement to detect the corrosion of reinforcement embedded in concrete. LUO et al<sup>[12]</sup> proposed a rebar corrosion monitoring device based on tapered polymer optical fiber sensor (TPFS). Some other indirect measurement schemes were also proposed to evaluate metal corrosion<sup>[13-16]</sup>.

Moreover, the processing of metal corrosion is exothermic reaction. And the heat emitted by metal corrosion may have bad effect to many affects. For example, a lithium ion battery (LIB) subjected to external heat may fail irreversibly<sup>[17]</sup>. A lithium ion battery (LIB) subjected to external heat may fail irreversibly. fiber optic sensors, especially fiber Bragg grating (FBG) sensors, attract intensive attention from researchers due to the unique

\* This work has been supported by the National Natural Science Foundation of China (Nos. 61835006 and 12274238).

\*\* E-mail: xiaoqiliu@nankai.edu.cn

advantages of high sensitivity and precision, satisfiable linearity, immunity to electromagnetic interference, resistance to harsh environments, light weight, small physical dimensions, easy-operability, and relatively low cost<sup>[18,19]</sup>. The FBG sensors, as the most commonly used fiber optic sensors, have been applied in many industries for the monitoring of strains, stress, loads, and temperatures<sup>[20,21]</sup>.

Mach-Zehnder interferometer (MZI) based on dislocation structure has been applied to refractive index sensing due to its high sensitivity and simple fabrication<sup>[22,23]</sup>. The refractive index sensitivity has been greatly improved due to the existence of U-shaped open cavity structure<sup>[24,25]</sup>. Metal corrosion is a trace change process, and a higher sensitivity interferometer is needed to achieve accurate monitoring. The open-cavity structure increases the sensitivity area with the environment, therefore, the sensitivity is also improved significantly.

In this paper, we propose a new scheme for metal electrochemical corrosion monitoring, the measurement is realized by an optical fiber sensor composed of a dislocation interferometer cascaded with an FBG. The relationship between optical fiber dislocation and transmission spectrum is also discussed by simulation. The temperature sensitivity of FBG and MZI is calibrated experimentally, and the transfer matrix of temperature and refractive index demodulation is obtained. The temperature changing of metal electrochemical reaction in different concentrations of NaCl solution at 1%, 3.5%, 5%, 10% and 20% is monitored by FBG. The changing of refractive index in the process of electrochemical corrosion at the concentration of 3.5% is investigated and the curve of refractive index changing is also obtained, which can characterize the corrosion process of metal.

The dislocation structure proposed in this paper is shown in Fig.1. The fibers A and C are on the same horizontal line, while the optical fiber B has dislocation in the radial direction, and the dislocation amount is  $d$ . Due to the introduction of optical fiber dislocation, the longer cavity length may introduce higher loss, and the designed cavity length is usually set to about 1 mm which may have much higher sensitivity<sup>[26]</sup>. The research in this paper is based on SMF. Based on the beam propagation method, we simulate the evolution of the electric field intensity of the light propagating in the optical fiber at different dislocation distances  $d$ . Fig.2 shows the beam propagation images of different dislocation amounts, such as 5.0  $\mu\text{m}$ , 30.0  $\mu\text{m}$  and 62.5  $\mu\text{m}$  when the cavity length  $L$  is set to 1 000  $\mu\text{m}$ . It can be seen that part of the intensity of light is leaked into the outer environment or the cladding and the transmission loss is increased with the increasing optical fiber dislocation. It should be noticed that nearly half of light is transmitted in the outer environment when the dislocation amount is 62.5  $\mu\text{m}$ . However, more light transmits in the outer environment, more information may be got by

the changing of the interference. Therefore, the dislocation amount is set to 62.5  $\mu\text{m}$ .

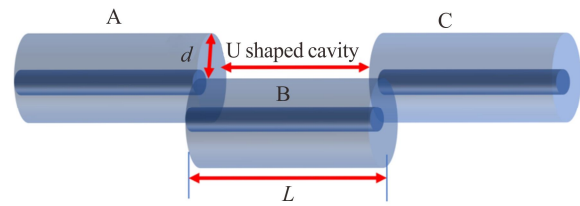


**Fig.1 Schematic diagram of optical fiber interferometer based on optical fiber dislocation structure**

Fig.3 shows the transmission spectrum with different dislocation amounts when the wavelength range is 1 300—1 600 nm and the interval of 1 nm. It can be seen that the transmission loss of the fiber is gradually increasing when the fiber dislocation is increasing, which is not conducive to beam propagation as we discussed above. When the dislocation amount is less than 30  $\mu\text{m}$ , there is no obvious interference peak in the transmission spectral line, because nearly no light is transmitted into the outer environment. With the increasing of  $d$ , more light is transmitted outside. It can be seen that there is an obvious interference peak, which is exactly what we want. Next, we discuss the interference sensitivity of the obtained transmission peak. As shown in Fig.3(b), when the optical fiber dislocation  $d$  is 62.5  $\mu\text{m}$ , the interference sensitivity reaches more than 13 000 nm/RIU. Thus, we have obtained an interferometer with high interference sensitivity, which is conducive to detecting small changes.

In our experiment, the MZI is fabricated by using commercial SMF28 (SMF-28e, Corning Inc, USA) and fusion splicer (Fujikura FSM-60s, Japan). First, the two standard SMF segments are spliced with a large lateral offset along the radial direction, and the offset distance is half of the optical fiber cladding. Then the 3D displacement optical platform is used to control the movement of the SMF to about 1 000 and then cut it off with a cutting knife. Finally, the optical fiber MZI interferometer can be obtained by controlling the optical fibers C and A segments on the same horizontal line and fusing them with the optical fiber B.

In our experiment, the refractive index and temperature sensitivity of the solution around the metal are important factors of MZI. Fig.4(a) is a schematic diagram of temperature measurement experimental setup. The temperature sensitivity and refractive index sensitivity of MZI are measured experimentally as shown in Fig.4(b)—(d). The proposed MZI is encapsulated in a microflow cell filled with ultrapure water. Light from a supercontinuum broadband source (SBS) is launched into the MZI, and the output interferometric transmission is monitored in real time by an OSA (Yokogawa: AQ6370C), with a wavelength resolution of 0.2 nm. The temperature range of the experiment is 25—60  $^{\circ}\text{C}$ , and the temperature interval is 2  $^{\circ}\text{C}$ . As shown in Fig.4(b) and (d), the refractive index

sensitivity of the interferometer of MZI with cavity length of  $L=947.02 \mu\text{m}$  is  $10\,500 \text{ nm/RIU}$ , which agrees well with theoretical numerical results. The measured temperature sensitivity is  $0.791\,6 \text{ nm/}^\circ\text{C}$ . Moreover, it can be seen

from Fig.4(d) that there is a narrow dip from  $1\,545 \text{ nm}$  to  $1\,550 \text{ nm}$ , which is induced by the FBG. This dip may help to mark the certain rank of interference fringe and avoid fringe skipping.

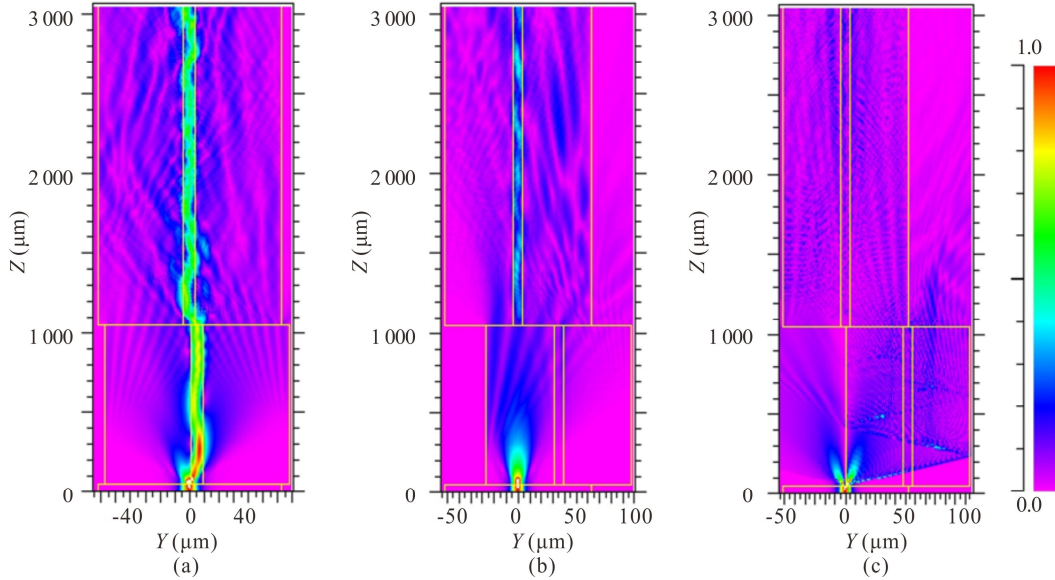


**Fig.2 Simulation results of fiber beam propagation process with different radial displacements: (a)  $d=5.0 \mu\text{m}$ ; (b)  $d=30.0 \mu\text{m}$ ; (c)  $d=62.5 \mu\text{m}$**

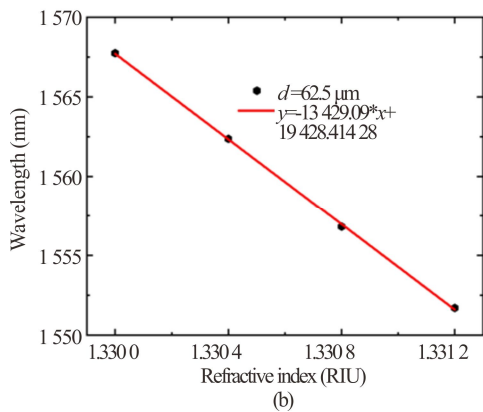
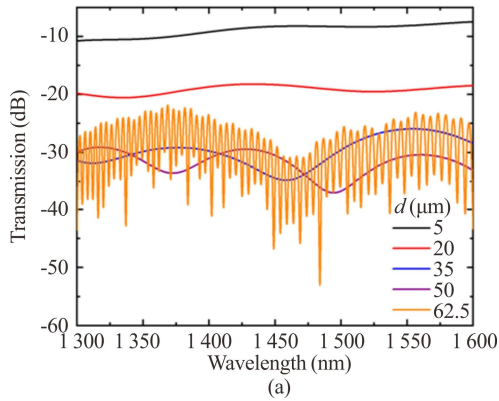


**Fig.3 (a) Transmission curves under different dislocations; (b) Simulated interference dip wavelength shift as a function of environmental refractive index**

Similarly, we calibrate the temperature sensitivity of FBG to demodulate the temperature effect of MZI later. The experimental range is set to  $28\text{--}64 \text{ }^\circ\text{C}$ , and the temperature interval is  $4 \text{ }^\circ\text{C}$ . The evolution of FBG transmission spectra is shown in Fig.5. Fig.5(b) is temperature sensitivity fitting curve of the FBG, and its temperature sensitivity is  $0.009\,29 \text{ nm/}^\circ\text{C}$ . So we can get the matrix of temperature and refractive demodulation.

$$\begin{pmatrix} \Delta\lambda_{\text{FBG}} \\ \Delta\lambda_{\text{MZI}} \end{pmatrix} = \begin{pmatrix} K_{T1} & K_{n1} \\ K_{T2} & K_{n2} \end{pmatrix} \begin{pmatrix} \Delta T \\ \Delta n \end{pmatrix}, \quad (1)$$

where  $K_{T1}$  and  $K_{T2}$  are the temperature sensitivities of FBG and MZI, respectively,  $K_{T1}=0.009\,29 \text{ nm/}^\circ\text{C}$ ,  $K_{T2}=0.791\,65 \text{ nm/}^\circ\text{C}$ .  $K_{n1}$  and  $K_{n2}$  are the refractive index sensitivities of FBG and MZI, respectively,  $K_{n1}=0$ . We can obtain

$$\Delta\lambda = \Delta\lambda_{\text{MZI}} - \frac{K_{T2}}{K_{T1}} \Delta\lambda_{\text{FBG}}, \quad (2)$$

where  $\Delta\lambda$  is the wavelength shift caused solely by changes in environmental refractive index,  $\Delta\lambda_{\text{MZI}}$  is the wavelength total shift of MZI, and  $\Delta\lambda_{\text{FBG}}$  is the wavelength shift of FBG.

Finally, an optical fiber sensor composed of an MZI cascaded with an FBG is used to monitor the metal corrosion process. The shift of wavelength is demodulated by Eq.(2) and used to characterize the changing of refractive index of solution in the process of metal corrosion. Fig.6 is a schematic of the experimental setup of the corrosion detection system.

Fig.7(a) shows that the temperature variation of metal electrochemical corrosion with 1%, 3.5%, 5%, 10% and 20% NaCl concentrations, which are obtained through temperature monitoring by the FBG. Fig.7(b) is the wavelength changing diagram of MZI with 3.5% NaCl concentration after temperature demodulation. 3.5%

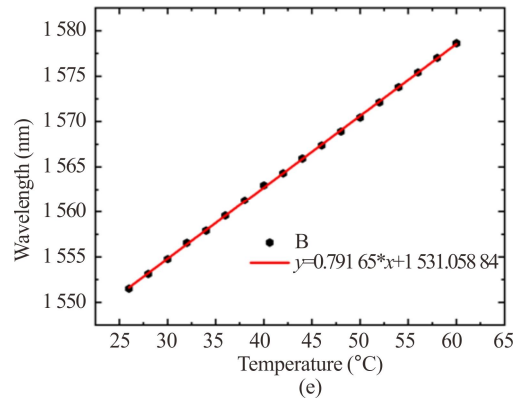
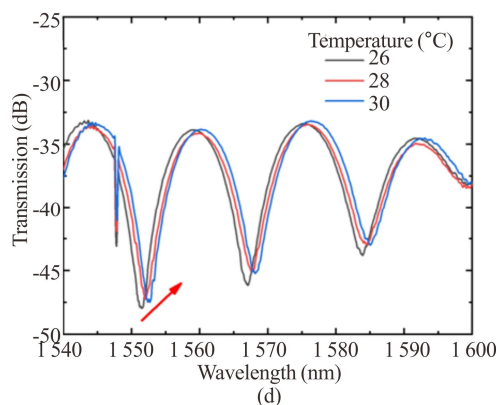
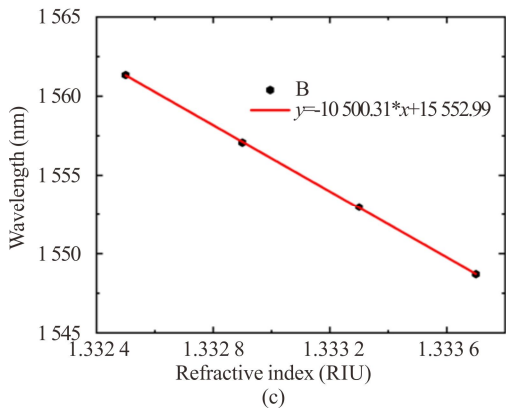
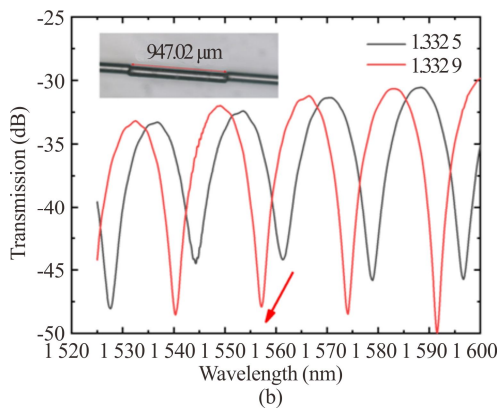
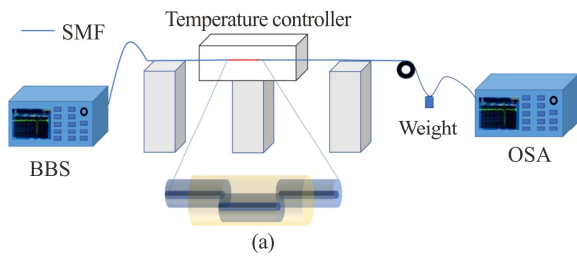


**Fig.4 (a) Schematic diagram of temperature measurement experimental setup; (b) Evolution of MZI transmission spectra under different refractive indices (The inset is a microscope image of MZI sensor with a U-shaped cavity length of 947 μm); (c) RI sensitivity fitting curve of MZI; (d) Evolution of transmission spectra of MZI in water at different temperatures; (e) Temperature sensitivity fitting curve of MZI**

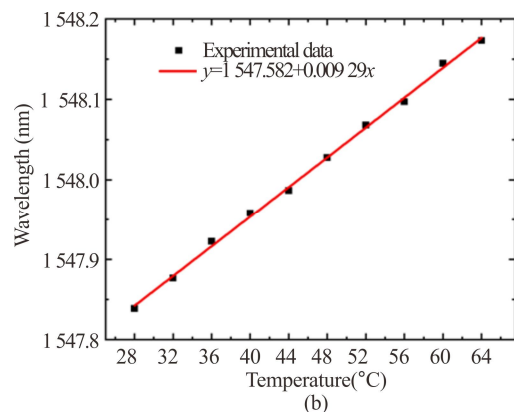
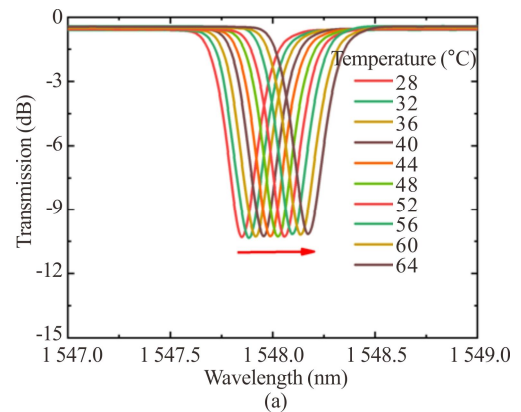


**Fig.5 (a) Evolution of FBG transmission spectra at different temperatures; (b) Temperature sensitivity fitting curve of FBG**

NaCl solution is quite similar to the concentration of seawater in nature, so it is used in our experiment as the corrosion solution. It can be seen that the initial corrosion rate of metal electrochemical corrosion process

gradually accelerates, and gradually slows down and stops with the increasing of corrosion time. It shows that the optical fiber sensor can monitor the metal corrosion under the conventional salt solution concentration.

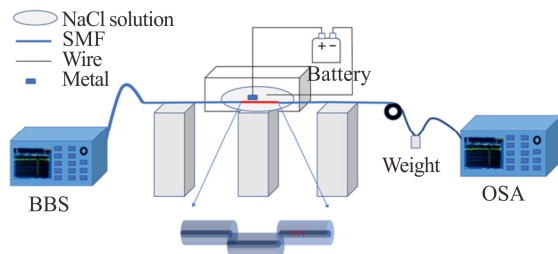


**Fig.6 Schematic of the experimental setup of the corrosion detection system**

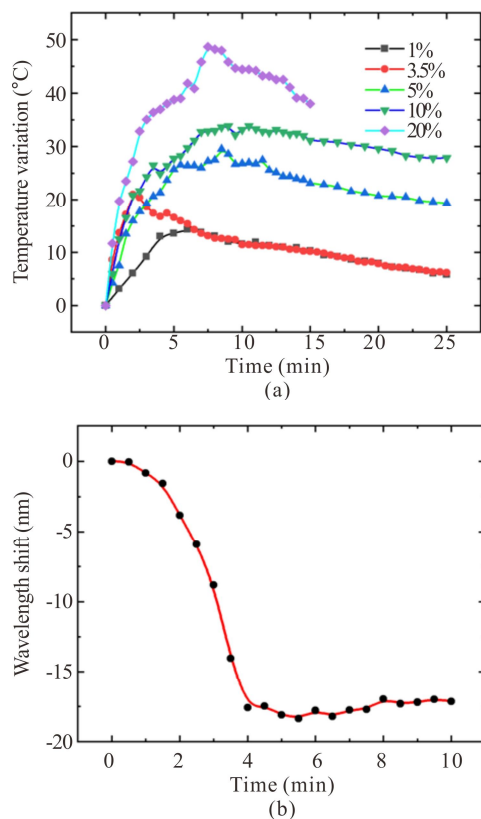


**Fig.7 (a) Temperature change diagram during electrochemical corrosion in NaCl solution with different concentrations; (b) Demodulated MZI wavelength change diagram at 3.5% NaCl concentration**

In summary, a fiber sensor composed of a dislocation MZI cascaded with an FBG is proposed, and it used to monitor the electrochemical reaction process of metals in experiments. The simulation results show that there will be obvious interference phenomenon when the fiber dislocation  $d > 30 \mu\text{m}$ . When  $d = 62.5 \mu\text{m}$ , its refractive sensitivity is above  $10\,000 \text{ nm/RIU}$ . An MZI with  $L = 947.02 \mu\text{m}$  has been fabricated experimentally, and its refractive index sensitivity is  $10\,500 \text{ nm/RIU}$ . Finally, the temperature of MZI is demodulated by the FBG, and the peak wavelength shift curve of MZI is obtained,

which characterizes the process of metal electrochemical corrosion. This setup may find applications in the corrosion of different kinds of metals and the monitoring of the electroplating process.

## Ethics declarations

## Conflicts of interest

The authors declare no conflict of interest.

## References

- [1] ZHAO X, GONG P, QIAO G, et al. Brillouin corrosion expansion sensors for steel reinforced concrete structures using a fiber optic coil winding method[J]. Sensors, 2011, 11: 10798-10819.
- [2] HU W, DING L, ZHU C, et al. Optical fiber polarizer with Fe-C film for corrosion monitoring[J]. IEEE sensors journal, 2017, 17: 6904-6910.
- [3] GUO C, FAN L, WU C, et al. Ultrasensitive LPFG corrosion sensor with Fe-C coating electroplated on a Gr/AgNW film[J]. Sensors and actuators B: chemical, 2019, 283: 334-342.
- [4] LAO J, SUN P, LIU F, et al. In situ plasmonic optical fiber detection of the state of charge of supercapacitors for renewable energy storage[J]. Light-science & applications, 2018, 7: 34.
- [5] WANG Y, SONG Y, XIA Y. Electrochemical capacitors: mechanism, materials, systems, characterization and applications[J]. Chemical society reviews, 2016, 45: 5925-5950.
- [6] ZHU C, GERALD R E, HUANG J. Ultra-sensitive microwave-photonic optical fiber interferometry based on phase-shift amplification[J]. IEEE journal of selected topics in quantum electronics, 2021, 27: 1-8.
- [7] BAO Y, HUANG Y, HOEHLER M S, et al. Review of fiber optic sensors for structural fire engineering[J]. Sensors (Basel), 2019, 19.
- [8] CHEN A H J, STRZODA R, FLEISCHER M, et al. Low-level and ultralow-volume hollow waveguide based carbon monoxide sensor[J]. Optics letters, 2010, 35.
- [9] TONG Z, WANG X, WANG Y, et al. Dual-parameter optical fiber sensor based on few-mode fiber and spherical structure[J]. Optics communications, 2017, 405: 60-65.
- [10] CHEN Y, TANG F, TANG Y, et al. Mechanism and sensitivity of Fe-C coated long period fiber grating sensors for steel corrosion monitoring of RC structures[J]. Corrosion science, 2017, 127: 70-81.
- [11] HOSHI Y, KOIKE T, TOKIEDA H, et al. Non-contact measurement to detect steel rebar corrosion in reinforced concrete by electrochemical impedance spectroscopy[J]. Journal of the electrochemical society, 2019, 166: 3316-3319.
- [12] LUO D, LI Y, LU T, et al. Tapered polymer optical fiber sensors for monitoring the steel bar corrosion[J]. IEEE transactions on instrumentation and measurement, 2021,

- 70: 1-9.
- [13] BARILLARO G, MERLO S, SURDO S, et al. Optical quality-assessment of high-order one-dimensional silicon photonic crystals with a reflectivity notch at  $\lambda \sim 1.55 \mu\text{m}$ [J]. *IEEE photonics journal*, 2010, 2: 981-990.
- [14] CARPIGNANO F, SURDO S, BARILLARO G, et al. Silicon micromachined device testing by infrared low-coherence reflectometry[J]. *Journal of microelectromechanical systems*, 2015, 2: 1960-1964.
- [15] NIEDZIAŁKOWSKI P, BIAŁOBRZESKA W, BURNAT D, et al. Electrochemical performance of indium-tin-oxide-coated lossy-mode resonance optical fiber sensor[J]. *Sensors and actuators B: chemical*, 2019, 301.
- [16] JANCZUK-RICHTER M, PIESTRZYŃSKA M, BURNAT D, et al. Optical investigations of electrochemical processes using a long-period fiber grating functionalized by indium tin oxide[J]. *Sensors and actuators B: chemical*, 2019, 279: 223-229.
- [17] LIU X, STOLIAROV S I, DENLINGER M, et al. Comprehensive calorimetry of the thermally induced failure of a lithium ion battery[J]. *Journal of power sources*, 2015, 280: 516-525.
- [18] XU L, ZHANG D, HUANG Y, et al. Monitoring epoxy coated steel under combined mechanical loads and corrosion using fiber Bragg grating sensors[J]. *Sensors (Basel)*, 2022, 22.
- [19] LOPEZ-HIGUERA J M, RODRIGUEZ C L, QUINTELA I A, et al. Fiber optic sensors in structural health monitoring[J]. *Journal of lightwave technology*, 2011, 29: 587-608.
- [20] HUANG S, HU X, ZHANG H, et al. A high-precision system of fiber Bragg grating temperature sensing demodulation based on light power detection[J]. *Optoelectronics letters*, 2022, 18: 461-467.
- [21] FAN X, JIANG J, ZHANG X, et al. Investigation on temperature characteristics of weak fiber Bragg gratings in a wide range[J]. *Chinese optics letters*, 2019, 17(12): 14-18.
- [22] TIAN Z, YAM S S H, LOOCK H P. Single-mode fiber refractive index sensor based on core-offset attenuators[J]. *IEEE photonics technology letters*, 2008, 20: 1387-1389.
- [23] CHEN J, ZHOU J, ZHANG Q, et al. All-fiber modal interferometer based on a joint-taper-joint fiber structure for refractive index sensing with high sensitivity[J]. *IEEE sensors journal*, 2013, 13: 2780-2785.
- [24] HU X, ZHANG H, WANG Y, et al. Magnetic-ionic-liquid-integrated microfiber Mach-Zehnder interferometer for simultaneous measurement of magnetic field and temperature[J]. *Optical fiber technology*, 2021, 67.
- [25] YI D, LIU F, GENG Y, et al. High-sensitivity and large-range fiber optic temperature sensor based on PDMS-coated Mach-Zehnder interferometer combined with FBG[J]. *Optics express*, 2021, 29: 18624-18633.
- [26] GONG T, LIU X, WANG Z, et al. A highly sensitivity humidity sensor based on mismatching fused fiber Mach-Zehnder interferometric without moisture material coating[J]. *Journal of optics*, 2020, 22(2): 025801.